ACI STRUCTURAL JOURNAL TECHNICAL PAPER

24-132

Shear Capacity of Composite Precast Prestressed Hollow-Core Slabs

by Deuckhang Lee, Min-Kook Park, Yuguang Yang, and Kang Su Kim

No practically viable method yet exists to provide minimum shear reinforcements into pretensioned precast hollow-core slab (PHCS) units produced through an automated extrusion method. Subsequently, the web-shear strength of PHCS units with untapped depths greater than 315 mm (12.5 in.) should be reduced in half, according to current ACI 318 shear design provisions. Meanwhile, continuous precast floor construction has been commonly adopted in current practices by using cast-in-place (CIP) topping and/or core-filling concrete. However, shear test results on continuous composite PHCS members subjected to combined shear and negative bending moment are very limited in literature. To this end, this study conducts shear tests of thick composite PHCS members with untapped depths greater than 315 mm (12.5 in.) and various span-depth ratios subjected to negative bending moments, where noncomposite and composite PHCS units subjected to shear combined with positive bending were also tested for comparison purposes. Test results show that flexure-shear strength can dominate the failure mode of continuous PHCS members rather than the web-shear failure, depending on the presence of CIP topping concrete and shear span-depth ratio. In addition, it was also confirmed that the shear strength of composite PHCS members is marginally improved by using a core-filling method under negative bending moment at continuous support, and thus its shear contribution seems not fully code-compliant and satisfactory to that estimated using ACI 318 shear design equations.

Keywords: composite action; continuous member; core-filling; flexure-shear; hollow-core slab; negative moment; shear strength; topping concrete; web-shear.

INTRODUCTION

Many commercial buildings, including parking structures, industrial factories, logistics warehouses, and residential buildings, were constructed using prestressed precast hollow-core slabs (PHCSs).[1-5] PHCS is generally applied as a simply supported precast concrete (PC) floor system or a continuous system (so-called half-PC method), as shown in Fig. 1, but because the role of the diaphragm in resisting the horizontal load during an earthquake as well as transmitting the vertical gravity action is considered important, a continuous system is preferred in construction practice to take advantage of its redundancy and better structural integrity.[6-9] In detail, as presented in Fig. 1, temporary loads during construction can be sustained solely by simply supported precast members with noncomposite precast section properties. Nonprestressed diaphragm and crack control reinforcements are then placed on top of the precast slab units, including the vicinity of the support regions for negative bending moment at the continuous intermediate support.[10,11] They can be properly integrated together using cast-in-place (CIP) topping concrete as composite prestressed concrete members.[12-15] This continuous composite floor system can minimize additional costs for temporary shores essentially required during construction. It is also very advantageous in deflection control and strength design under service and ultimate loading conditions by using composite section properties with CIP topping concrete,[12] where its design flexural moments can be significantly reduced in the midspan by achieving span continuity at interior supports (refer to Fig. 2).

According to Clause 7.6.3.1 in the current ACI 318 Code,[16] the design web-shear strength of PHCS with untapped depth (h) greater than 315 mm (12.5 in.) should be reduced by half (that is, $\phi V_{cw}/2$ rule), because the minimum area of shear reinforcement ($A_{v,min}$) cannot be directly provided in PHCS units due to its automated fabrication process to form multiple hollow cores in the section (that is, extrusion method, shown in Fig. 3).[1-5] Therefore, some concerns are being raised in practices regarding the safe shear design of thick PHCS members.[1-5,7,17-20] To this end, extensive shear tests were conducted on thick PHCS members, and some viable shear-strengthening methods, such as the core-filling method, have been examined in previous studies to improve the web-shear strength of a simply supported PHCS member at its end regions within the transfer length (l_t). The core-filling method has been shown to enhance shear capacity significantly, where the voids (hollow cores) of PHCS are filled by CIP concrete combined with shear reinforcements. Some existing studies conducted by Palmer and Schultz,[18,19] McDermott and Dymond,[21] Asperheim and Dymond,[22] Lee et al.,[2,4] and Kim et al.[23] also confirmed the practical applicability of this approach, emphasizing the critical role of composite action among the core-filling concrete, shear reinforcement integrated with topping concrete, and the PHCS units in achieving code-compliant shear strength. These findings highlight the importance of core-filling as a practical and efficient strategy to improve the shear performance of PHCS members, where the web-shear capacity usually dominates the design strength and failure mechanism.[16,24]

On the other hand, this study is strongly motivated by the observation that flexure-shear strength (V_{ci}) can govern the behavior near the intermediate supports of continuous

ACI Structural Journal, V. 122, No. 6, November 2025.

MS No. S-2024-132.R2, doi: 10.14359/51748928, received February 19, 2025, and reviewed under Institute publication policies.

(a) Simple support system

(b) Continuous support system (half-PC method)

Fig. 1—Support conditions in current construction practices.

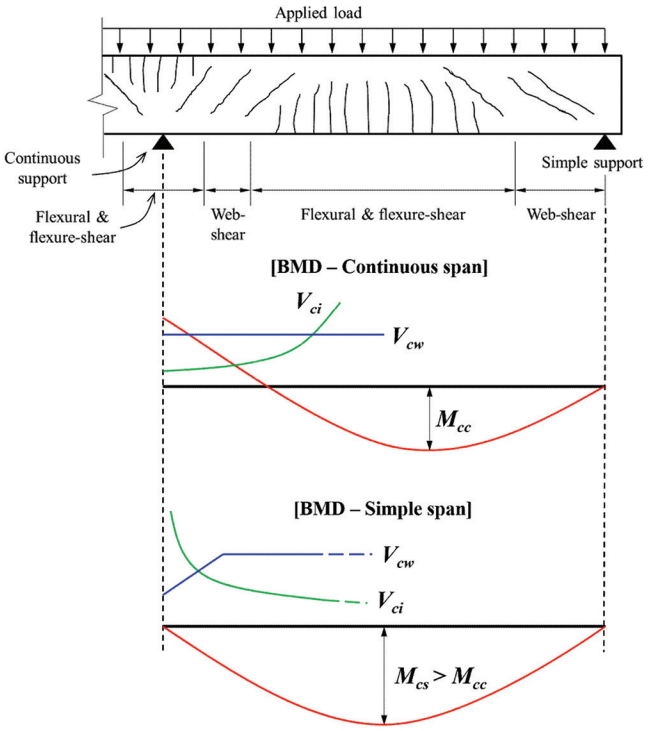

Fig. 2—Effect of end-continuity and shear cracking pattern (reproduced from Fig. R22.5.6.3 in ACI 318-19[17]).

PHCS floor systems rather than web-shear strength (that is, $V_{cw} \geq V_{ci}$), as shown in Fig. 2. The continuity with the core-filling and CIP topping concrete induces substantial negative moment at the intermediate support, significantly reducing the flexure-shear capacity. It also makes flexure-shear strength (V_{ci}) critical in determining the shear strength of composite PHCS members. In addition, while several studies including Corney et al.[25] and Sarkis et al.[26] investigated the seismic performance and negative bending behavior of continuous composite PHCS members, almost no experimental data on the shear strength of continuous systems under gravity loads is available in literature. In particular, shear testing is still required on a PHCS member strengthened by the core-filling method subjected to negative bending moment combined with gravity shear for the application of continuous PHCS flooring system. In this study, the shear strengths of noncomposite (that is, with no CIP topping concrete) and composite PHCS members with various loading conditions (that is, positive or negative bending moment combined with shear) are experimentally investigated, including a composite PHCS specimen strengthened in shear by using the core-filling method combined with shear reinforcements which are anchored to the longitudinal reinforcement in the CIP topping concrete. On this basis, this study aims at examining the applicability of the shear design provision of the prestressed composite member specified in the current ACI 318 building code considering the various design options.

RESEARCH SIGNIFICANCE

Continuous flooring systems have been adopted in the current practices of the precast construction industry to achieve continuities at interior supports. The main concerns of existing studies were generally focused on the web-shear strength of thick PHCS members under simply supported conditions due to a long-lasting critical issue regarding the minimum shear reinforcement provision addressed in ACI 318 to avoid size effect issues (so-called $\phi V_{cw}/2$ rule). In this study, the shear strengths of thick PHCS composite members subjected to negative bending moment were experimentally evaluated for the first time to identify the effect of loading conditions, large shear-span depth ratio, and presence of CIP-topping and/or core-filling concretes as key testing variables. Finally, the applicability of current ACI code-compliant shear design methods was examined in detail.

CONTINUOUS PRECAST CONSTRUCTION IN PRACTICE

Figures 3(a) and (b) show a typical fabrication process of individual noncomposite PHCS units in a prestressing long-line bed of precast factory, and Fig. 3(c) and (d) show its actual field construction for a continuous precast flooring system using PHCS members. As depicted in Fig. 3(a), because PHCS units are typically produced by the extrusion method by using extremely dry concrete, it is very difficult to provide any shear reinforcement and also to address a roughened surface (irregularity), even right after casting on the top of PHCS units, as required in ACI 318-19[16] for proper composite performances (refer to Clause 16.4 of

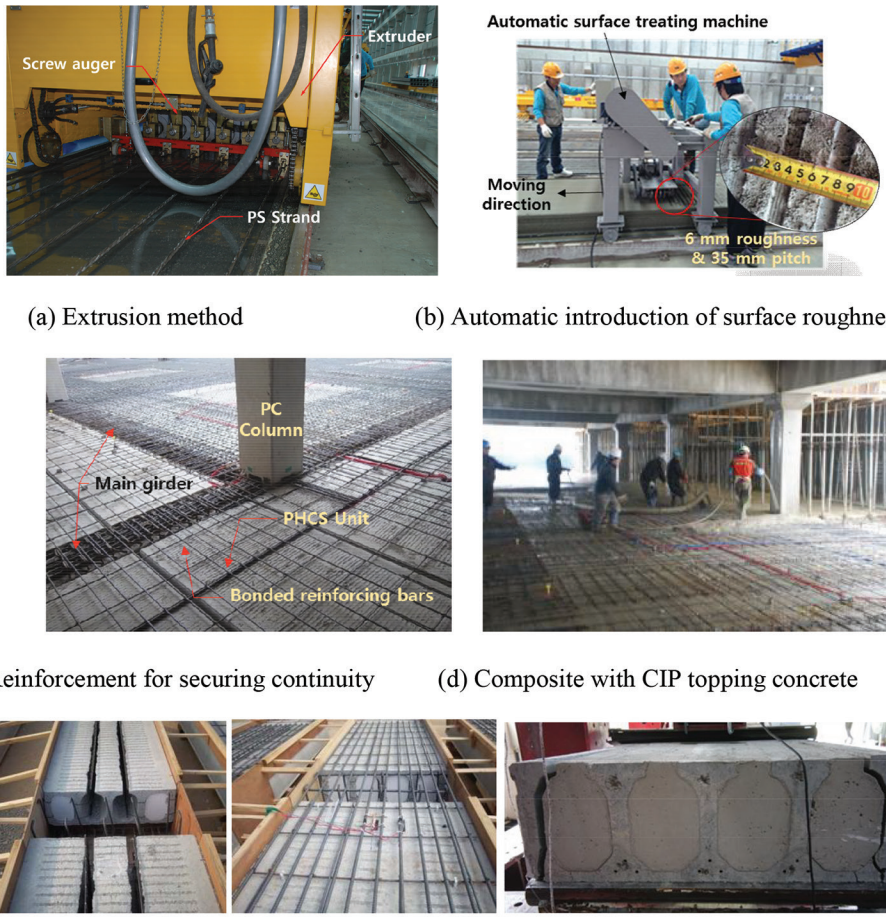

(a) Extrusion method

(b) Automatic introduction of surface roughness

(c) Reinforcement for securing continuity

(d) Composite with CIP topping concrete

(e) Fabrication of test specimens

Fig. 3—Fabrication and construction of PHCS floor system.

ACI 318-19). Therefore, so-called intentionally roughened condition with 35 mm (1.18 in.) spacing and 6 mm (0.24 in.) depth on the top surface of precast hollow-core planks was addressed perpendicular to the longitudinal direction by using an automated sawing machine, as shown in Fig. 3(b). On this basis, composite performance between PHCS and CIP topping concrete can be properly secured. Note that it was clearly confirmed from the authors' previous study[1-4] through direct shear tests that the aforementioned roughness condition introduced on the surface of PHCS units can fully satisfy the minimum requirement of horizontal shear performance specified in ACI 318 (that is, $v_{nh} >$ 0.56 MPa [80 psi]). The individual PHCS units are then cut into a target length by using movable cutting equipment, and final individual precast units are temporarily stored in the factory yard until on-site delivery. After the main precast frame system is installed on site, as shown in Fig. 3(c), PHCS units are erected and installed under a simply support condition, usually on inverted-tee girders and column corbels (if any), and are then integrated by using CIP topping concrete in which additional nonprestressed reinforcements are provided as diaphragm, shrinkage, and temperature-control reinforcements. Self-weight and construction loads including topping concrete are supported solely by the simply supported PHCS units, while service and factored loads are designed to be resisted by the topped composite PHCS section with continuous support condition. In addition, as described in Lee et al.,[2] the core-filling method is frequently adopted in practice to improve the web-shear strength of a thick PHCS with a depth greater than 315 mm (12.5 in.) within the transfer length (l_t). In this case, for better constructability, as presented in Fig. 3(e), some portions of the top flanges are partially removed right after casting using a diamond saw, by which the CIP concrete can be easily filled into some selected hollow cores. Shear reinforcement greater than the minimum amount of shear reinforcement (that is, $A_v \geq A_{v,min}$) can also be placed in CIP core-filling concrete, thereby ensuring improved structural integrity and a stronger composite action. Note that the shear reinforcements need to be tightly anchored to longitudinal reinforcements in CIP topping concrete for the successful application of the core-filling method.[24]

SHEAR DESIGN PROVISION OF PHCS MEMBERS SPECIFIED IN ACI 318

According to the so-called approximate method specified in the current ACI 318-19 building code,[16] the shear strength of prestressed flexural members can be calculated when the effective prestress force exceeds 40% of the tensile strength of flexural reinforcements—that is, $A_{ps}f_{se} \geq 0.4(A_{ps}f_{pu} + A_sf_y)$, as follows

$$V_{c,simp} = \left(0.05\lambda\sqrt{f_c'} + 4.8\frac{V_u d_p}{M_u}\right) b_w d \quad (1)$$

where f_c' is the compressive strength of concrete; A_{ps} and A_s are the areas of prestressed and nonprestressed longitudinal tension reinforcements, respectively; f_{pu} and f_y are the tensile strength of prestressed reinforcement and yield strength of nonprestressed reinforcement, respectively; λ is the reduction factor for lightweight concrete; V_u and M_u are the factored shear and moment at considered section; b_w is the width of web concrete; d is the distance from extreme compression fiber to centroid of longitudinal tension reinforcements (refer to Eq. (4)); d_p is the distance from extreme compression fiber to centroid of prestressed reinforcement, which cannot be taken as $0.8h$ in applying Eq. (1); and h is the member thickness. In addition, Eq. (1) need not be taken less than $0.17\lambda\sqrt{f_c'}b_w d$ nor greater than $0.42\lambda\sqrt{f_c'}b_w d$. According to Clauses 22.5.6.1 and 22.5.7.3 specified in ACI 318,[17] the shear strength of pretensioned members estimated by Eq. (1) within its transfer length (l_t) shall not exceed the web-shear strength (V_{cw}) presented later in Eq. (3), where L_t is taken to be $50d_{bp}$ and d_{bp} is the diameter of a prestressing strand. This means that the shear strength of simply supported PHCS members is usually governed by web-shear strength. The effective depth of prestressing strands (d_p) can be clearly defined for PHCS members with a straight profile. However, as presented outside of the parentheses in Eq. (1), it is unclear in ACI 318-19 how the effective depth of longitudinal tension reinforcement (d) should be defined for negative bending moments[27-30]; it can be defined based on the centroid of the reinforcement areas or that of tensile strength (d_A or d_F), respectively, as follows

$$d_A = \frac{A_s d_s + A_p d_p}{A_s + A_p} \quad (2a)$$

$$d_F = d = \frac{f_y A_s d_s + f_{se} A_p d_p}{f_y A_s + f_{se} A_p} \quad (2b)$$

In this study, the effective depth defined by Eq. (2b) is adopted based on Bondy and Bondy (that is, $d = d_F$),[30] where f_{se} is the magnitude of effective prestress. Meanwhile, ACI 318-19 also permits to take the shear strength of prestressed members by using the so-called detailed method as the lesser of flexure-shear and web-shear strengths—that is, $V_c = \min(V_{ci}, V_{cw})$, in which the flexure-shear strength (V_{ci}) can be estimated as follows

$$V_{ci} = 0.05\lambda\sqrt{f_c'}\, b_w d_p + V_d + \frac{V_i M_{cre}}{M_{max}} \quad (3)$$

where V_d is the unfactored shear force due to dead load (usually due to total self-weight of prestressed member plus CIP topping concrete); V_i and M_{max} are the factored shear force and flexural moment occurring simultaneously at section due to externally applied loads (that is, excluding the effect of dead load); M_{cre} is the moment causing flexural cracking at section due to externally applied loads, which can be taken as $(I/y_t)\left(0.5\lambda\sqrt{f_c'} + f_{pe} - f_d\right)$; and f_{pe} and f_d are the compressive stress in concrete due to effective prestressing forces and stress due to unfactored dead load, respectively, at extreme fiber of section where tensile stress is caused by externally applied loads (extreme top fiber for the case under negative bending). In addition, the flexure-shear strength estimated from Eq. (3) does not need to be smaller than $0.17\lambda\sqrt{f_c'}\, b_w d$ when $A_{ps}f_{se} \geq 0.4(A_{ps}f_{pu} + A_s f_y)$. Otherwise, it needs not be taken less than $0.14\lambda\sqrt{f_c'}\, b_w d$. The web-shear cracking strength (V_{cw}) can be determined[13] as follows

$$V_{cw} = \left(0.29\lambda\sqrt{f_c'} + 0.3f_{pc}\right) b_w d_p + V_p \quad (4)$$

where f_{pc} is the compressive stress occurring at the centroid of section due to prestress; V_p is the vertical component of effective prestressing force at section; and d_p needs not be taken less than $0.8h$ for Eq. (3) and (4). In addition, it should also be noted that the current ACI 318-19 specifies that the minimum shear reinforcement should be provided if the factored shear force (V_u) exceeds the half of the design web-shear strength ($0.5\phi V_{cw}$) for the hollowed-section members with untopped depth exceeding 315 mm (12.5 in.). This means that the design web-shear strength of PHCS units tested in this study should be taken as half of that estimated from Eq. (4), because all the specimens tested in this study contained no shear reinforcement.

No clear and straightforward design expression is available for estimating shear strength of composite precast members in current design code, but Clause 22.5.4.3 in ACI 318-19[16] stipulates that the shear strength of a composite member with nonuniform section properties can be calculated by using properties of the individual components or by using the critical property of a component resulting in the smallest shear strength. This provision can be interpreted as the shear strength of a composite member can be taken as the sum of shear contributions provided from prestressed precast member and nonprestressed (CIP topping concrete) component (that is, $V_c = V_{pc} + V_{CIP}$) or as the smallest one between those two components (that is, $V_c = \min[V_{pc}, V_{CIP}]$).[31-33] Note that V_{pc} is the shear contribution of a PC unit estimated from Eq. (1) or the lesser of Eq. (3) and (4), and V_{CIP} is that provided by CIP topping and core-filled concrete. The former method can be defined as simple summation method (SSM), and the latter can be named critical strength method (CSM). In addition, Clause 22.5.4.4 in ACI 318-19 presents that shear strength can be estimated by assuming a monolithically cast member, and it indicates that the transformed section property can be used in calculating the shear strength of a composite precast member. The computation of shear strength is much more cumbersome when the PHCS member is strengthened with CIP topping and core-filled concrete. This approach is defined in this study as transformed section approach (TSA). Figure 4 shows schematic descriptions of those design approaches, based on ACI 318 shear design provisions.[16] A total of six possible combinations of the shear strength estimation methods can be considered as follows

$$\text{CSM 1: } V_{n1} = V_{c1} + V_s = \min[\min(V_{ci}, V_{cw}), V_{CIP}] + V_s \quad (5)$$

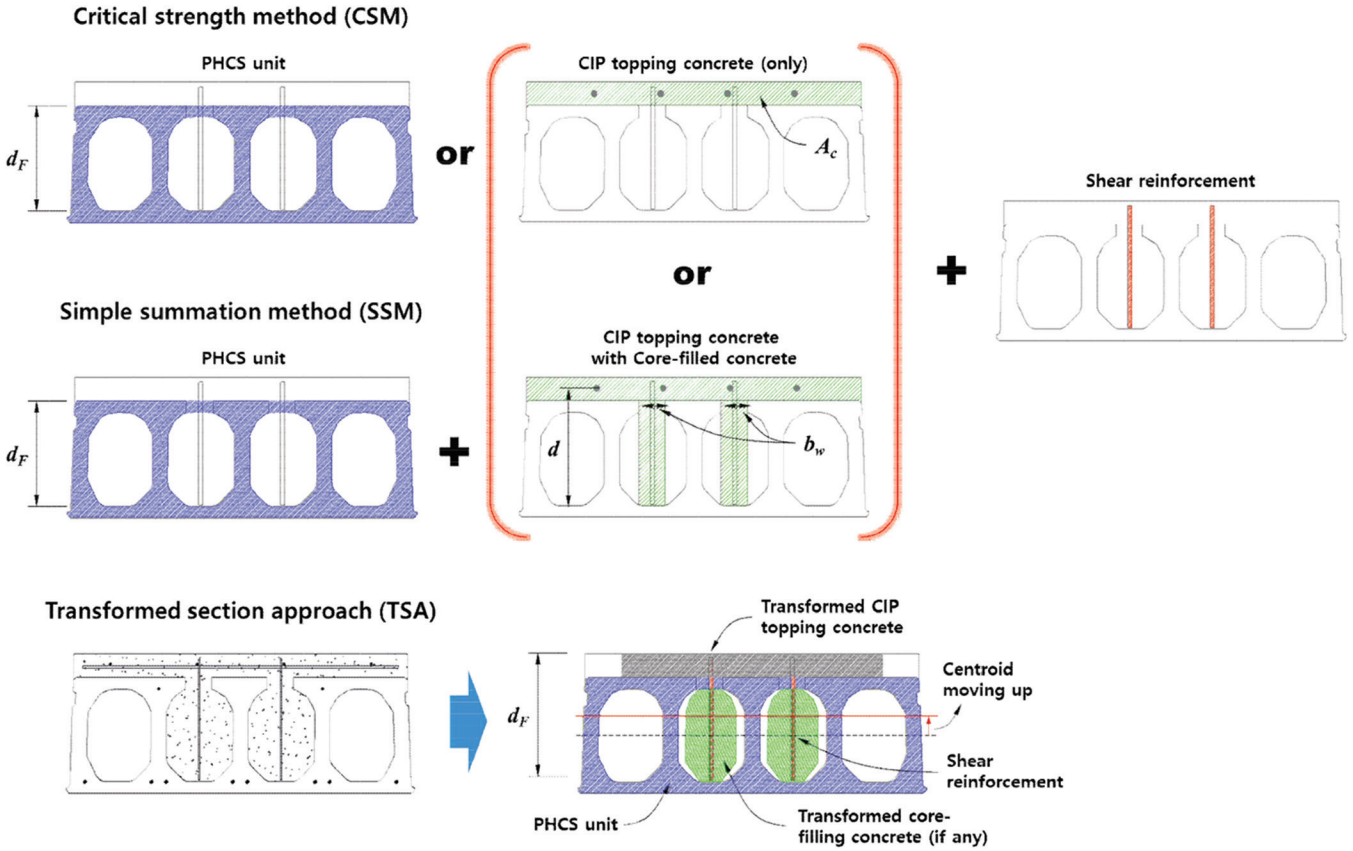

Fig. 4—Description of code-compliant design methods.

$$\text{CSM 2: } V_{n2} = V_{c2} + V_s = \min[V_{c,simp}, V_{CIP}] + V_s \quad (6)$$

$$\text{TSA 1: } V_{n3} = V_{c3} + V_s = \min(V_{ci}, V_{cw}) + V_s \text{ with transformed section properties} \quad (7)$$

$$\text{TSA 2: } V_{n4} = V_{c4} + V_s = V_{c,simp} + V_s \text{ with transformed section properties} \quad (8)$$

$$\text{SSM 1: } V_{n5} = V_{c5} + V_s = \min(V_{ci}, V_{cw}) + V_{CIP} + V_s \quad (9)$$

$$\text{SSM 2: } V_{n6} = V_{c6} + V_s = V_{c,simp} + V_{CIP} + V_s \quad (10)$$

where V_{CIP} is the shear strength of CIP nonprestressed concrete. For the composite PHCS members reinforced only with topping concrete (that is, CP, CN, and CN-5 specimens in this study, to be explained in the next section), because the minimum shear reinforcement is not provided ($A_v < A_{v,min}$), V_{CIP} should be estimated using $0.66\lambda\rho_w^{1/3}\sqrt{f_c'}b_w d$, where the longitudinal reinforcement ratio (ρ_w) is taken as the sum of the areas of longitudinal bars located more than two-thirds of the overall member depth away from the extreme compression fiber, according to Commentary R22.5.5.1 of ACI 318-19. On this basis, there is no valid longitudinal reinforcement for the CP, CN, and CN-5 specimens for which V_{CIP} is taken to be zero in this study. For this reason, V_{c1} and V_{c2}, defined in Eq. (5) and (6), respectively, are calculated using a value determined from $\min(V_{ci}, V_{cw})$ and $V_{c,simp}$, respectively. On the other hand, for the PHCS members reinforced in shear with both the topping and core-filled concrete (that is, CN-F specimen in this study to explained in the next section), V_{CIP} which is taken as $0.17\lambda\sqrt{f_c'}b_w d$ for CSM and SSM approaches according to the shear strength of nonprestressed member with the minimum shear reinforcement ($A_v \geq A_{v,min}$) specified in Eq. (a) of Table 22.5.5.1 in ACI 318-19. Note that b_w is taken to be the minimum web width (refer to Fig. 4), and the effective depth (d) is the distance between the extreme compression fiber to centroidal axis of longitudinal reinforcements pin topping concrete.

As shown in Fig. 2 and 4, for a simply supported condition under positive bending moment, because the critical section is located within the transfer length (that is, $l_t > h/2$), the corresponding magnitude of prestress is far less than the effective prestress (f_{se}) at the critical section and thus the web-shear strength usually dominates the failure mechanism of a PHCS member. In addition, the stress and force terms in Eq. (2) can be estimated in a relatively simple manner. As presented in Eq. (2), because V_{ci} expression considers the effect of dead load (V_d) including self-weight apart from externally applied loads and section properties before and after composite with CIP topping concrete, its computational procedures to estimate all force and stress terms are heavily cumbersome for the case of composite members. In more detail, the transformed section property (TSA 1 and TSA 2) can be obtained based on the elastic modulus ratio between precast prestressed member and CIP topping concrete ($n = E_{c,cip}/E_{c,pc}$), and it affects the section properties (I and y_t) including the subsequent stress terms f_{pc}, f_{se}, and f_d of V_{cw} and V_{ci} presented in Eq. (1), (3), and (4). Note that $E_{c,cip}$ and $E_{c,pc}$ are the elastic modulus of concrete used in CIP and PHCS units, respectively. On the other hand, it is believed

that the critical strength and simple summation methods are straightforward and simple to be applied in estimating the shear strength of composite PHCS members subjected to combined loads. However, it is clear to be quite conservative and is doubtful in the shear contribution of topping concrete in tension. Thus, to this end, following simple alternative approaches can be considered

$$\text{Alternative 1: } V_{n7} = V_{c7} + V_s = V_{c,simp} + V_s, \text{ where core-filling concrete is ignored} \quad (11)$$

$$\text{Alternative 2: } V_{n8} = V_{c8} + V_s = \left(0.17\lambda\sqrt{f_c'}\, b_{w,comp}\, d_p\right) + V_s \quad (12)$$

where Alternative 1 is basically the same as the TSA-2 method except that the effect of core-filling concrete is ignored in the computation for a purpose of simplification and safe shear design. For Alternative 2, as mentioned, because the effective prestress (f_{se}) approaches zero value at the end region, the section properties are transformed into homogeneous nonprestressed concrete sections by assuming no prestressing effect. This method is quite a common approach used in current practices as a conservative design method for the shear design of pretensioned members at the end region. Note that V_c is taken as $0.17\lambda\sqrt{f_c'}$ in Eq. (12) based on the minimum shear strength of prestressed member as specified in Clause 22.5.6.2 of ACI 318-19.

EXPERIMENTAL PROGRAM

Test specimens

The experimental program is divided into two testing groups: 1) PHCS subjected to shear combined with positive bending (that is, simply supported condition); and 2) PHCS subjected to shear combined with negative bending (continuous-support condition). All the PHCS units used in this study were commercially available products and were fabricated using the extrusion method from a commercial precast plant operated in South Korea. Their dimensional details and material properties are presented in Fig. 5 and Table 1, respectively. A total of seven specimens were fabricated and tested in this study, where the untopped thickness of all the noncomposite PHCS units were 400 mm (15.7 in.). Thus, the so-called $0.5\phi V_{cw}$ rule specified in Clause 7.6.3.1 of ACI 318-19 (that is, the minimum shear reinforcement provision of one-way slab) should be applied in estimating web-shear strengths ($\because h \geq 315$ mm [12.5 in.]). For composite specimens, the total thickness of the composite section was 480 mm (18.9 in.) including 80 mm (3.15 in.) thick CIP topping concrete. As presented in Table 1, the first letter of each specimen ID refers to the presence of CIP topping concrete, where N and C are the noncomposite and composite members (that is, presence of topping concrete), respectively. Note that the same tests were conducted on three noncomposite PHCS units subjected to positive bending to get more reliable results. The next letter denotes loading configurations, where P and N indicate the application of positive and negative flexural moment combined with shear force, respectively (that is, simple or continuous support condition). The last nomenclature is optional only for the composite specimens subjected to negative bending moment, and this additional letter was used only for two composite specimens out of three CN-series specimens, which refers to the presence of core-filling concrete (CN-F specimen) and relatively large shear span-depth ratio (a/d) compared to other specimens (CN-5 specimen). In summary, the test program included three identical PHCS specimens with no topping concrete subjected to positive bending (NP-series specimens), one composite PHCS specimen subjected to positive bending (CP specimen), and three composite PHCS specimens subjected to negative bending in which the testing variables are a/d and presence of core-filling concrete (CN-series specimens). More details can be found in Tables 1 and 2.

As mentioned previously, all noncomposite PHCS units, including those used for the composite specimens (C-series specimens), were cut from an 80 m (262.5 ft) long original member in the same batch of a long-line prestressing bed. This fact indicates that the noncomposite precast planks with 400 mm (15.75 in.) thickness (that is, untopped depth) had almost the same dimensions and homogeneous material properties, where eight 12.7 mm (0.5 in.) and two 9.5 mm (0.37 in.) seven-wire low-relaxation strands were provided in their precompression zone and another side, respectively. All the prestressing strands were pretensioned simultaneously with a straight profile, as shown in Fig. 3. The magnitude of the effective prestress (f_{se}) was measured at 1209 MPa (175.3 ksi), and its specified tensile strength (f_{pu}) was 1860 MPa (270 ksi). As presented in Table 1, the magnitudes of the compressive stresses at the centroid of the precast concrete section due to prestress (f_{pc}) before composite with CIP topping concrete was 5.11 MPa (0.74 ksi), and those estimated at the centroid of the composite sections ranged from 3.33 to 5.11 MPa (0.48 to 0.74 ksi), and more detailed information can be found in Appendix A.* For the composite specimen under positive moment (that is, CP specimen), D10 reinforcements (No. 3) with 300 mm (11.8 in.) spacing were provided in CIP topping concrete under compression. For other composite specimens subjected to negative bending (CN series), D16 (No. 5) deformed reinforcing bars for CN and CN-5 were provided in CIP topping concrete with 100 mm (3.94 in.) spacing, and corresponding reinforcement ratio ($\rho_s = A_s/bd_s$) was approximately 0.46%, where b is the flange width of PHCS units.

Installation, measurement, and testing setup

As shown in Fig. 5(a), three identical NP-series specimens were tested under simply supported condition to investigate the web-shear strengths of thick noncomposite PHCS units under positive moment within the transfer length (l_t), and those results were previously reported in Lee et al.[2] As mentioned previously, the remaining four specimens (C-series specimens) had the same dimension and material properties as the NP-series specimen except for the presence of

*The Appendix is available at **www.concrete.org/publications** in PDF format, appended to the online version of the published paper. It is also available in hard copy from ACI headquarters for a fee equal to the cost of reproduction plus handling at the time of the request.

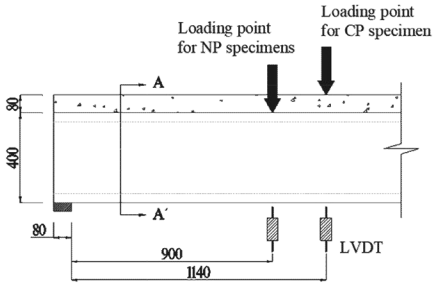

(a) Test setup – NP and CP specimens

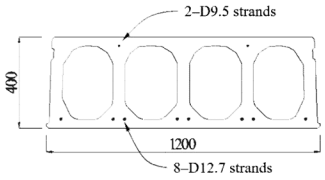

(b) cross-section of NP specimens

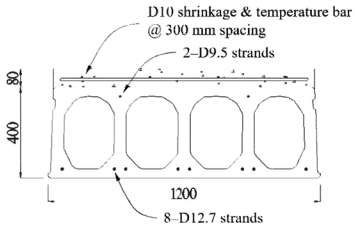

(c) cross-section of CP specimens

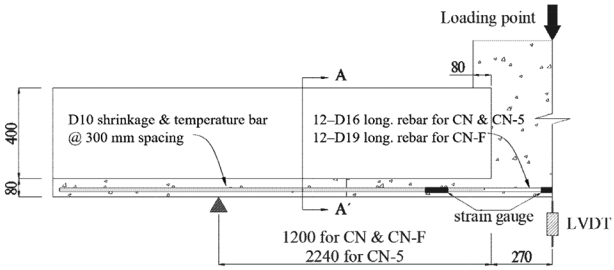

(d) Test setup – CN, CN-5 and CN-F specimens

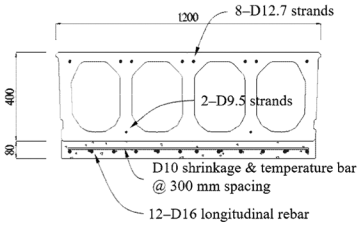

(e) cross-section of CN and CN-5 specimens

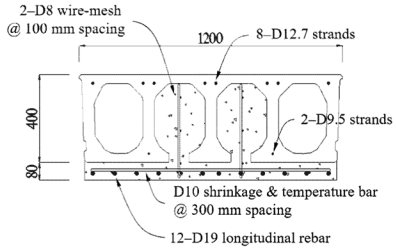

(f) cross-section of CN-F specimen

Fig. 5—Dimensional details of test specimens. (Note: 1 mm = 0.039 in.)

CIP topping concrete with 80 mm (3.15 in.) thickness or core-filled concrete (if any) combined with shear reinforcements. The NP and CP specimens under positive bending were tested in the end region within the transfer length (l_t), where the effective prestress (f_{se}) was not fully developed. Among the C-series specimens, only the CP specimen was subjected to positive moment; otherwise, negative bending moment was applied under the pseudo-continuous support condition (refer to Fig. 5(b)). To this end, as presented in Fig. 3(g), two PHCS units 2.0 m (6.56 ft) in length were installed on a reinforced concrete (RC) inverted T-beam in the same way as used in practical precast construction at 5 days after casting precast members by using the extrusion method. Then, nonprestressed reinforcements were placed on the top of PHCS units, and those were integrated using CIP topping concrete. Twenty-eight days after casting CIP topping concrete, it was carefully flipped upside down to apply negative bending moment under the same testing setup used in the N-series specimens. The specimens were then carefully installed on supports in the loading frame to place CIP topping concrete to be on the tension side due to external loading and PHCS units to be on the top side (refer to Fig. 5(b)), where the transfer length of the CN series was located near the loading point (that is, maximum moment region). As shown in Fig. 6, a single point load was applied to all test specimens using a 1000 kN (220 kip) capacity actuator under displacement control, and the loading rate was set to be 0.025 mm/s (9.84×10^{-4} in./s). It should be noted that the a/d of the CN-5 specimen was 5.0 to investigate flexure-shear strength. For other specimens, their a/d was set to be 2.6, and it was expected that web-shear mechanism would dominate their failure mode. Meanwhile, core-filled concrete was applied with shear reinforcements only to CN-F specimen (refer to section details shown in Fig. 5(f)).

Table 1—Dimensional and material properties of test specimens

	Concrete		Geometry											Longitudinal reinforcement			
			PHCS unit					CIP concrete (topping and core-filling)									
	$f_{c,PHCS}'$	$f_{c,CIP}'$	h_{PHCS}	b_w	b_{core}	d_p	f_{pc}	$h_{comp.}$	A_{core}	d_F	a/d_F	$y_{b,comp.}$	$I_{comp.}$	A_{ps}	$A_{s,CIP}$	ρ_p	$f_{pc,comp.}$
Specimen ID	MPa	MPa	mm	mm	mm	mm	MPa	mm	mm^2	mm	—	mm	mm^4	mm^2	mm^2	%	MPa
NP1	60.5	—	400	276	—	360	5.11	—	—	360	2.6	198	4,407,825,763	900	—	0.244	—
NP2																	
NP3																	
CP	60.5	28.3	400	276	—	360	5.11	480	—	440	2.5	259	7,578,090,830	900	285	0.244	3.33
CN	60.5	28.3	400	276	—	360	5.11	480	—	430	2.6	221	7,578,090,830	900	2383	0.026	3.33
CN-5	60.5	28.3	400	276	—	360	5.11	480	—	430	5.0	221	7,578,090,830	900	2383	0.026	3.33
CN-F	60.5	28.3	400	276	450	360	5.11	480	129869	433	2.6	237	8,502,640,495	900	3438	0.026	3.79

Note: Three identical specimens were fabricated and tested for NP-series specimens; first letter of specimen ID: N is noncomposite, C is composite; second letter of specimen ID: P is positive moment, N is negative moment; 1 mm = 0.039 in.; 1 MPa = 0.145 ksi.

Table 2—Key matrix of test program

Comparator (C) / Reference (R)	CP specimen (C/R)*	CN-5 specimen (C/R)*	CN-F specimen (C/R)*
NP-series	Topping concrete (1.03)	—	—
CN specimen	Support condition (0.73)	Span-depth ratio (0.47)	Core-filling concrete (1.16)

*C/R: is ratio of shear test result (comparator/reference).

Note that the CN-F specimen was reinforced in shear using D10 (No. 3) stirrups with 300 mm (11.8 in.) spacing within the core-filling concrete, as shown in Fig. 5(f) and Table 1, to satisfy the minimum shear reinforcement provision specified in ACI 318-19. The corresponding shear reinforcement ratio (ρ_v) was 0.025% based on the total width after composite with core-filled concrete as $A_v/(b_{wp} + b_{core})s$, where b_{wp} and b_{core} are the web width of the PHCS unit and core-filling concrete, respectively. Because all the shear reinforcements were provided in the core-filling concretes, not directly in precast PHCS unit, strictly speaking, it does not fully satisfy the aforementioned minimum shear reinforcement provision.

The vertical deformations of the specimens were measured at the loading point during testing and strain gauges were installed in the nonprestressed reinforcement, as shown in Fig. 5. But no strain gauge could be installed in the prestressing strands due to tight production schedules in the commercial precast plant under day-to-day operations. Table 3 shows the mixture proportions of the dry concrete used for the precast PHCS units, which is optimized for the extrusion process where those of CIP topping concretes used as topping and core-filling concretes were also presented. The water-cement ratio (w/c) of the dry concrete mixture was 36.2%, and the maximum aggregate size was 13.0 mm (0.5 in.). Almost zero slump was observed from fresh concrete. The design strength of concrete used in precast members was 40.0 MPa (5.8 ksi), while the average concrete compressive strength of the PHCS ($f_{c,PC}'$) obtained at the day of testing was 60.5 MPa (8.7 ksi). The average compressive strength of the CIP topping concrete ($f_{c,CIP}'$) used for the topping and core-filling materials was 28.4 MPa (4.1 ksi) on the day of testing.

EXPERIMENTAL RESULTS

As shown in Table 2, by comparing NP and CP specimens, the influence of CIP topping concrete on the web-shear strengths of simply supported PHCS members subjected to positive moments can be evaluated. Additionally, the effect of the support conditions (or negative bending) on the shear strength of PHCS members can be justified from the comparison of test results observed from CP and CN specimens. Furthermore, the impact of the a/d on the shear strength of continuous PHCS members subjected to negative bending moment can be evaluated by comparing the shear strengths of the CN and CN-5 specimens. Finally, by comparing the CN and CN-F specimens, the effectiveness of the core-filling method combined with shear reinforcements can be experimentally validated.

Effect of CIP topping concrete on PHCS members subjected to positive bending moment

All the noncomposite PHCS specimens showed typical web-shear cracking failure modes, as shown in Fig. 7, where critical web-shear cracks can be clearly observed across the shear spans. Those specimens showed almost identical and linear responses and failed right after the sudden web-shear cracking, resulting in no post-peak response. As shown in Fig. 7 and Table 3, the average shear strength of the NP-series specimens was estimated at 279.0 kN (62.7 kip), and the strength variation among them was less than 10%. Their shear strengths were substantially higher than the web-shear capacity estimated by the ACI web-shear strength method presented in Eq. (4), even with no consideration of the $\phi V_{cw}/2$ rule specified in Clause 7.6.3.1 of the current ACI 318 Code for thick PHCS members, which indicates no critical issue on the so-called size effect in the PHCS specimens with a member depth greater than 315 mm (12.4 in.). Figure 7 shows the test results of the CP specimen with topping concrete under positive bending moment, which is basically identical with NP-series specimens except for the presence of CIP topping concrete. The CP specimen showed

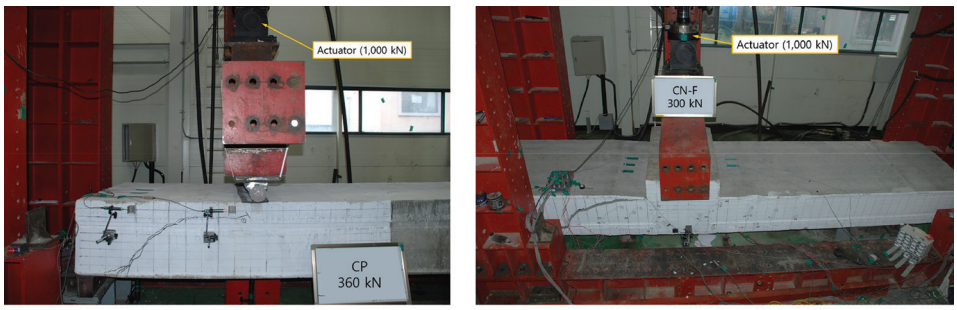

(a) CP specimen (b) CN-F specimen

Fig. 6—Test setup and failure mode of CP and CN-F specimens.

Table 3—Concrete mixture design used for test specimens

Mixture proportion		*w/c*, %	*S/a*, %	W, kg/m^3	Unit weight, kg/m^3		
					C	S	G
PHCS	13-40-000	36.2	34.9	160	340	683	1268
CIP	25-24-150	47.5	48.8	160	337	868	909

Note: *S/a* is sand-to-total aggregate ratio; 1 mm = 0.039 in.; 1 MPa = 0.145 ksi; 1 kg/m^3 = 0.0624 lb/ft^3; 1 kg = 2.204 lb.

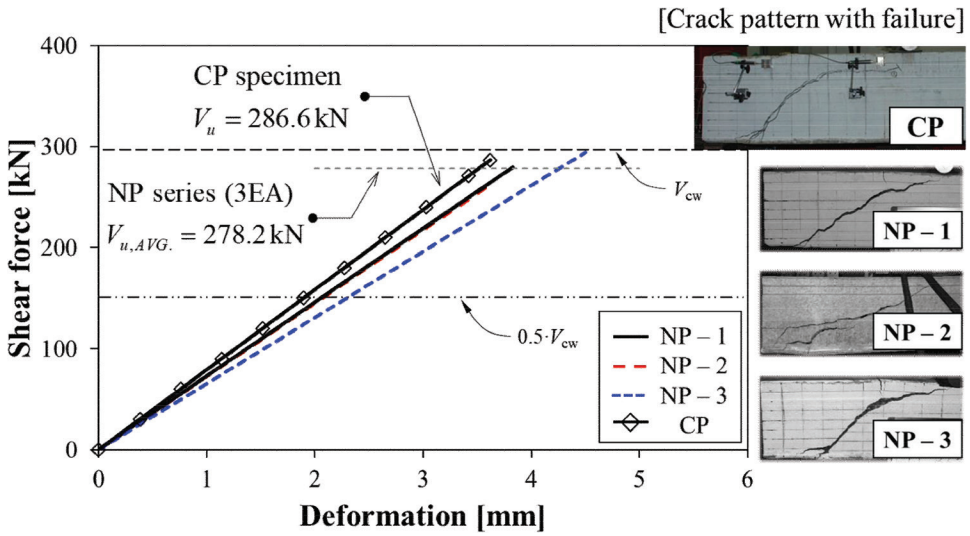

Fig. 7—Shear force-deformation response and crack pattern of NP-series and CP specimen. (Note: 1 mm = 0.039 in.; 1 kN = 0.2248 kip.)

higher flexural stiffness compared to the NP series as expected, and overall response was quite similar with those of the NP specimens. At a shear force of 286.6 kN (64.4 kip), diagonal shear cracking was observed in the precast unit, at which sudden web-shear failure occurred. As seen in the NP specimens, no post-cracking behavior was observed. It also appeared that the shear contribution of CIP topping concrete was marginal, and the shear strength increase of the CP specimen compared to the NP specimens (that is, provided from topping concrete) was limited under 10% of the shear strength of concrete estimated from the ACI 318 Code model for nonprestressed component (that is, $V_{CIP} = 0.17\lambda\sqrt{f_c'}b_w d$). Surely, the shear strength of the CP specimen is higher than web-shear strength (V_{cw}) estimated from Eq. (4) of ACI 318 with no application of the $0.5\phi V_{cw}$ rule from the minimum shear reinforcement provision.

Effect of negative bending moment on composite PHCS members

Figures 8 and 9(a) show the test results and cracking pattern of the CN specimen subjected to negative bending moment. At shear force of 120 kN (26.9 kip), multiple flexural cracks were observed near the interior support. Then, critical shear cracking developed on the concrete web first and finally propagated into the compression zone and CIP topping concrete in tension at a shear force of 392 kN (88.1 kip), after which there was no post-peak response. The shear stiffness of the CP and CN specimens were almost identical to each other as compared in Fig. 8, but the shear strength of the CN specimen was approximately 40% greater than the PHCS specimen subjected to positive bending moment (that is, CP specimen). It indicates that the failure of the CN specimen was triggered by web-shear mechanism because the estimated web-shear strength was substantially greater than

flexure-shear strength (that is, $V_{cw} \geq V_{ci}$) at the critical section located at $h/2$ away from the loading point (refer to Fig. 5). Figure 9(a) presents the strain response measured from the nonprestressed reinforcement in CIP topping concrete under tensile stress, which was far less than its yield strain ($\varepsilon_y = f_y/E_s$). It also indicates that the shear strength of the CN specimens was governed by web-shear failure mode.

The test results of the CN-F specimen with core-filling concrete and shear reinforcements are presented in Fig. 8, and Fig. 9(b) shows its cracking pattern observed at shear failure. The overall shear response of this specimen is quite similar to the previous CN specimen with the same a/d, but many clear horizontal shear cracks appeared in the CN-F specimen along the interface between PHCS and CIP topping concrete. This means that a significant effect of flexure was in the response of the CN-F specimen reinforced by core-filling concrete and shear reinforcements compared to the CN specimen with no core-filling concrete. Shear failure was finally triggered by shear, where a critical shear crack finally propagated into both the compression and tension zones. Meanwhile, as shown in Fig. 10(b), unlike the CN specimen, the tensile strain response of the CN-F specimen measured from the nonprestressed reinforcements provided in CIP topping concrete reached almost the yield strain level, and clear post-peak response was also observed. In addition, the transverse reinforcement did not yield. This indicates that the flexure-shear mechanism strongly affected the failure mode. More evidence can also be found from the fact that the shear strength was measured at 455 kN (102.3 kip), and this shear force was just 16.1% greater than that of the CN specimen with no core-filling concrete. Thus, the contribution of CIP concrete and shear reinforcements is marginal compared to that calculated from the ACI method (that is, $V_{CIP} + V_s = 0.17\sqrt{f_c'}b_w d + A_v f_y d/s$) and thus not fully reliable when it comes to flexure-shear mechanism. Though, from the shear force-deformation response presented in Fig. 10(a), the effectiveness of core-filling concrete can be confirmed considering that the main purpose of the minimum shear reinforcement provision is to achieve enough reserved deformational capacity (that is, post-peak response) and additional strength to avoid brittle failure right after shear cracking, as explained in Park et al.,[34] Lee and Kim,[35] and Teoh et al.[36]

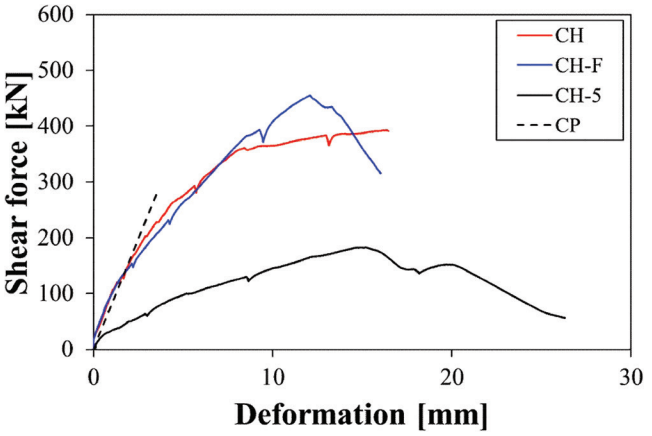

Fig. 8—Shear force-deformation response and crack pattern of composite specimens. (Note: 1 mm = 0.039 in.; 1 kN = 0.2248 kip.)

The shear force-displacement response of the CN-5 specimen with the highest shear span-depth ratio (that is, a/d = 5.0), is shown in Fig. 8. Several flexural cracks were initiated near the loading point at shear force equal to 70 kN (15.7 kip), and then horizontal shear crack was observed in the middle of shear span at 135 kN (30.3 kip). This horizontal interface crack was merged with the existing diagonal shear crack and finally propagated into the compression zone and edge of RC inverted T-beam in the middle span, as shown in Fig. 9(c). In addition, the critical shear crack separated the interface between the PHCS unit and CIP topping concrete, which indicates the flexure-shear mechanism dominated the failure mode. As shown in Fig. 10(c), compared to the CN specimen, the magnitude of tensile strains measured from the nonprestressed reinforcements provided in CIP topping

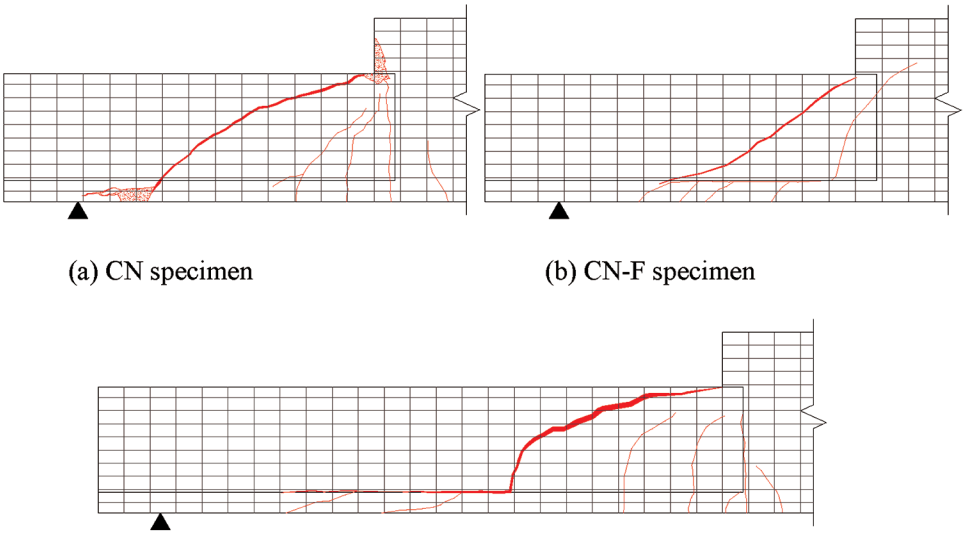

Fig. 9—Crack patterns of C-series specimens.

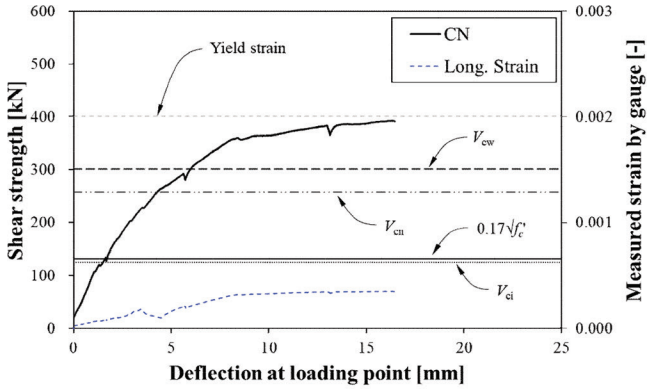

(a) CN specimen

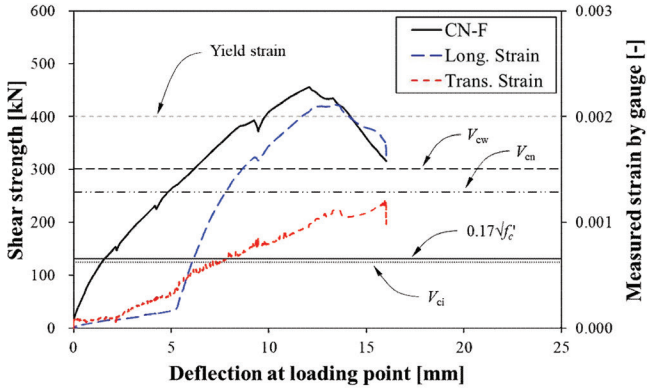

(b) CN-F specimen

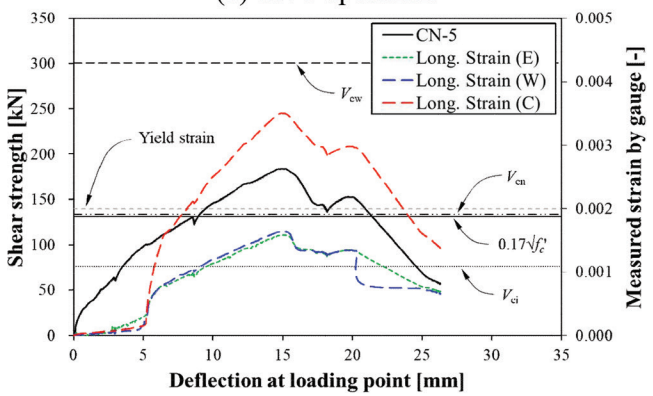

(c) CN-5 specimen

Fig. 10—Strain responses of test specimens. (Note: 1 mm = 0.039 in.; 1 kN = 0.2248 kip.)

concrete was substantially higher, and one clearly yielded, as well. This fact indicates that the shear transfer mechanism of the CN-5 specimen was dominated by the flexure-shear strength due to its large *a*/*d*. It also appeared that the observed strength of the CN-5 specimen is greater than the shear strength of concrete estimated using conventional RC members specified in ACI 318 (that is, $v_c = 0.17\sqrt{f_c'}$), but it was clearly less than the concrete contribution term in the web-shear strength model of prestressed concrete ($v_c = 0.29\sqrt{f_c'}$; refer to Eq. (4)). This affirms again that the shear failure of the CN-5 specimen was triggered by the flexure-shear mechanism.

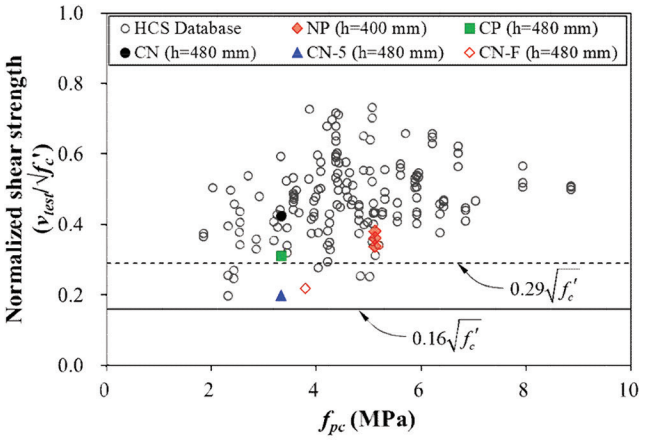

(a) Effect of prestress

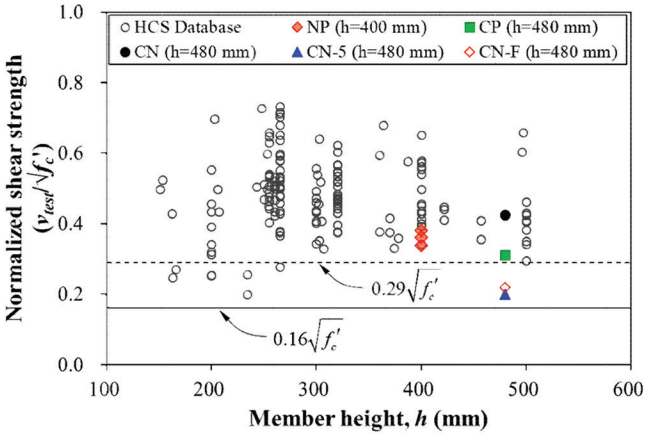

(b) Effect of member depth

Fig. 11—Comparison of test results with existing shear database. (Note: 1 MPa = 0.145 ksi; 1 mm = 0.039 in.)

EVALUATION OF TEST RESULTS

ACI 318 detailed and simple method

The shear strength of the PHCS members with no CIP topping concrete can be calculated in a relatively simple manner. In addition, contrary to Hawkins and Ghosh's concerns,[17] even for the PHCS members with no minimum shear reinforcement, the web-shear strength estimated from the current ACI 318 Code presented in Eq. (4) is still conservative even without reducing the web-shear strength by half (that is, when the minimum shear reinforcement provision was ignored). This trend can be confirmed from Fig. 11, where existing web-shear test results of PHCS units were compared with those reported in this study. Note that the detailed information of the collected specimens is presented in Table 4. For the case of the composite PHCS members tested in this study, a subsequent calculation process in their shear strengths was extremely cumbersome and complex, as pointed out by Lee et al.,[27] Ju et al.,[28] Kang et al.,[29] and Bondy and Bondy.[30] This point can also be found in Appendix A.

Figure 12 and Table 5 show comparisons between the test results of the composite PHCS specimens and those estimated by several code-compliant design approaches

Table 4—Dimensions and material properties of collected PHCS test specimens

Reference: Authors (Year)	No. of specimens	Void type*	f_c', MPa	h, mm	b_w, mm	f_{pc}, MPa	ρ_p, %	a/d_F	V_{test}, kN
Walraven and Mercx[37]	19	C & I	13.8 to 51.1	255 to 300	255 to 300	2.5 to 5.9	0.7 to 1.5	1.7 to 6.7	182 to 286
Pajari[38]	50	C & I	38.1 to 63.7	200 to 500	215 to 335	1.8 to 7.0	0.7 to 2.0	1.7 to 6.7	80 to 528
TNO[39]	39	C & I	59.9 to 113.9	255 to 400	241 to 449	3.6 to 8.8	0.9 to 2.6	2.9 to 3.2	224 to 652
Bertagnoli and Mancini[40]	14	I	55.0 to 65.7	163 to 422	335 to 444	2.3 to 6.8	0.4 to 1.1	2.8 to 4.5	97 to 478
University of L'Aquila[41]	14	C & I	58.1	151 to 497	215 to 414	2.0 to 5.7	0.6 to 1.1	2.7 to 3.7	157 to 714
Celal[42]	8	C	62.9 to 67.9	206 to 305	229 to 313	3.6 to 5.0	1.0 to 1.5	3.0 to 3.8	163 to 297
Rahman et al.[43]	5	C	40.0	250 to 300	316 to 325	4.7 to 5.3	0.9	2.3 to 2.8	199 to 299
Simasathien and Chao[44]	2	I	36.2	457	203	3.2	0.7	2.7	182 to 209
Palmer and Schultz[19]	24	I	53.9 to 68.7	305 to 508	300 to 439	1.0 to 5.5	0.6 to 1.3	2.5 to 4.0	221 to 610
Park et al.[3]	10	C & I	60.5	200 to 500	242 to 300	2.5 to 3.1	0.7 to 1.2	2.5 to 3.1	82 to 454

*Void type: C is circle, I is irregular.

Note: 1 mm = 0.039 in.; 1 MPa = 0.145 ksi; 1 kN = 0.2248 kip.

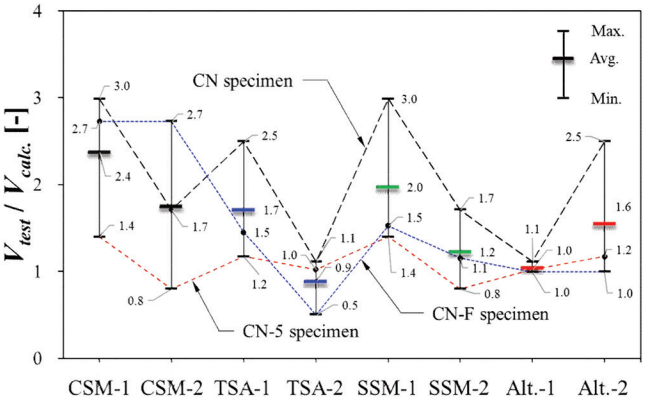

Fig. 12—Comparison of test results with code-compliant analysis methods.

presented in Eq. (5) to (12). In the case of the CSM, the second method showed a more straightforward calculation process for composite PHCS members, and the individual shear contribution of each CIP topping concrete component (for example, topping concrete or core-filling concrete, if any) was found to be negligible compared to that of PHCS members.

On the other hand, when the TSA is adopted, the shear strength of concrete is significant. For the case of the web-shear strength, the strength increase can be explained by an increase in the effective depth of composite section (d), while for the case of flexure-shear strength, it is increased by the cracking moment term (M_{cre}). In the case of the SSM, the shear strengths of the specimens were overall estimated in unsafe side. The shear strength of composite PHCS with core-filling concrete and shear reinforcements (CN-F specimen) showed an increase in shear strength of 16.1% compared to that with no core-filling concrete (CN specimen), but this observed strength increase was clearly less than its shear contribution calculated from code-compliant methods, as presented in Fig. 12. Thus, the Alternative 1 method expressed in Eq. (11), in which the influence of core-filling concrete is neglected, provided excellent analysis results. Meanwhile, the Alternative 2 method presented in Eq. (12), where the influence of prestress is ignored to take advantage of simplified calculations, provides conservative analysis results. Based on a simpler calculation process compared to other methods, it is believed that the approximate equation ($V_{c,simp}$) shown in Eq. (1) can be used as the shear strength evaluation equation for composite PHCS members. Because it ignores composite action in strength computations, shear strength can be easily calculated and has shown to provide safety results. However, there was a limitation as it could not be applied in the end region of pretensioned members because the minimum prestress magnitude condition does not usually satisfy $A_{ps}f_{se} < 0.4(A_{ps}f_{pu} + A_sf_y)$.

CONCLUSIONS

1. It was experimentally confirmed that the shear resistance mechanism of continuous prestressed hollow-core slab (PHCS) members subjected to negative bending can be governed by the flexural-shear cracking strength rather than web-shear failure, depending on shear span-depth ratio and presence of core-filling concrete.

2. Web-shear strengths of PHCS members with a thickness of 400 mm (15.75 in.) were found to sufficiently exceed the web-shear strength provided by the current ACI 318 Code, which indicates that the web-shear strength reduction requirement of PHCS members not reinforced in shear ($0.5\phi V_{cw}$ rule) could be stringent.

3. The shear strength of composite PHCS with core-filling concrete and shear reinforcements showed an increase in shear strength of approximately 20% compared to that with no core-filling concrete, but this increase appeared far less than its shear contribution calculated from code-compliant methods. On this basis, for simplified and safe shear design, it can be recommended that the shear contribution of core-filling concrete is ignored in computation of shear strength

Table 5—Summary of test and analysis results

Specimens	V_{test}, kN	V_{test}/V_{n1}	V_{test}/V_{n2}	V_{test}/V_{n3}	V_{test}/V_{n4}	V_{test}/V_{n5}	V_{test}/V_{n6}	V_{test}/V_{n7}	V_{test}/V_{n8}
CP	286.6	2.18	1.25	0.82	0.74	0.90	1.25	0.74	1.78
CN	392.5	2.99	1.71	2.50	1.11	2.99	1.71	1.11	2.50
CN-5	183.7	1.40	0.80	1.17	1.02	1.40	0.80	1.02	1.17
CN-F	455.7	2.73	2.73	1.45	0.50	1.53	1.15	0.99	1.00
AVG	—	2.32	1.62	1.48	0.85	1.70	1.23	0.97	1.61
SD	—	0.61	0.71	0.63	0.24	0.78	0.32	0.14	0.59
COV	—	0.26	0.44	0.42	0.28	0.46	0.26	0.14	0.37

Note: 1 kN = 0.2248 kip.

of composite PHCS sections subjected to high negative bending moment, presented as Alternative design methods in Eq. (11) and (12).

4. ACI 318 stipulates no clear and straightforward design method for composite PHCS members. Thus, several design options can be considered and this study presented various possible design combinations. On this basis, it appeared that simple summation methods provide conservative results, while other methods are too cumbersome to be used in practice. To this end, this study presents several design alternatives, and it appeared that Alternative 1 provides a good level of accuracy with a simple calculation process.

AUTHOR BIOS

ACI member **Deuckhang Lee** *is an Associate Professor in the Department of Architectural Engineering at Chungbuk National University, Cheongju, Korea. He received his BS, MS, and PhD from the University of Seoul, Seoul, Korea. He is a member of Joint ACI-ASCE Committee 550, Precast Concrete Structure, and ACI Subcommittees 445-E, Shear and Torsion – Torsion, and 445-F, Shear and Torsion – Interface Shear.*

Min-Kook Park *is a Research Professor in the Department of Architectural Engineering at the University of Seoul. He also serves in a research position at Delft University of Technology (TU Delft), Delft, the Netherlands. He received his PhD from the University of Seoul. His research interests include the shear design of reinforced, precast, and prestressed concrete members.*

ACI member **Yuguang Yang** *is an Associate Professor in the Department of Engineering Structures at TU Delft. He is a member of ACI Subcommittee 445F, Shear and Torsion – Interface Shear. His research interests include shear in concrete structures.*

Kang Su Kim *is a Professor in the Department of Architectural Engineering at the University of Seoul. He received his BS and MS in architectural engineering from Inha University, Incheon, Korea, and his PhD from the University of Illinois Urbana-Champaign, Urbana, IL. His research interests include advanced technology in concrete structures.*

ACKNOWLEDGMENTS

This work was supported by the National Research Foundation of Korea (NRF) grant funded by the Korean government (MSIT) (No. RS-2023-00209647 and RS-2023-00220019). The authors would also like to give sincere thanks to Samsung C&T Corporation for supporting this work by the project K2012-07, "Developments of Enhancement Techniques on Shear Strength of Hollow-Core Slab and Its Composite Action with Topping Concrete."

REFERENCES

1. Park, M. K.; Lee, D. H.; Yang, Y.; Zhang, D.; and Kim, K. S., "Composite Performance of Prestressed Hollow-Core Slabs with Cast-in-Place Concrete Topping," *ACI Structural Journal*, V. 119, No. 4, July 2022, pp. 153-164.

2. Lee, D. H.; Park, M. K.; Ju, H. E.; Han, S. J.; and Kim, K. S., "Strengths of Thick Prestressed Precast Hollow-Core Slab Members Strengthened in Shear," *ACI Structural Journal*, V. 117, No. 2, Mar. 2020, pp. 129-140.

3. Park, M. K.; Lee, D. H.; Han, S. J.; and Kim, K. S., "Web-Shear Capacity of Thick Precast Prestressed Hollow-Core Slab Units Produced by Extrusion Method," *International Journal of Concrete Structures and Materials*, V. 13, No. 1, 2019, pp. 1-14.

4. Lee, D. H.; Park, M. K.; Oh, J. Y.; Kim, K. S.; Im, J. H.; and Seo, S. Y., "Web-Shear Capacity of Prestressed Hollow-Core Slab Unit with Consideration on the Minimum Shear Reinforcement Requirement," *Computers and Concrete*, V. 14, No. 3, 2014, pp. 211-231.

5. Lee, D. H.; Park, M. K.; and Kim, K. S., "Current Issue on Shear Design of Deep Prestressed Hollow-Core Slabs," The 2019 World Congress on Advances in Structural Engineering and Mechanics (ASEM19), Jeju Island, Korea, 2019.

6. Corney, S. R.; Henry, R. S.; and Ingham, J. M., "Performance of Precast Concrete Floor Systems during the 2010/2011 Canterbury Earthquake Series," *Magazine of Concrete Research*, V. 66, No. 11, 2014, pp. 563-575.

7. Corney, S. R.; Ingham, J. M.; and Henry, R. S., "Seismic Testing of Support Connections in Deep Hollow-Core Floor Units," *ACI Structural Journal*, V. 115, No. 3, May 2018, pp. 735-748.

8. Iverson, J., and Hawkins, N., "Performance of Precast/Prestressed Concrete Building Structures during Northridge Earthquake," *PCI Journal*, V. 39, No. 2, 1994, pp. 38-55.

9. Fleischman, R. B.; Naito, C. J.; Restrepo, J.; Sause, R.; and Ghosh, S. K., "Seismic Design Methodology for Precast Concrete Diaphragms, Part 1: Design Framework," *PCI Journal*, V. 50, No. 5, 2005, pp. 68-83.

10. Zhang, D.; Fleischman, R.; and Lee, D. H., "Verification of Diaphragm Seismic Design Factors for Precast Concrete Office Buildings," *Earthquakes and Structures*, V. 20, No. 1, 2021, pp. 13-27.

11. Zhang, D.; Fleischman, R.; and Lee, D. H., "Effects of Diaphragm Flexibility on the Seismic Design Acceleration of Precast Diaphragms," *Computers and Concrete*, V. 25, No. 3, 2020, pp. 273-282.

12. Elliott, K. S., "Research and Development in Precast Concrete Framed Structures," *Progress in Structural Engineering and Materials*, V. 2, No. 4, 2000, pp. 405-428.

13. Zhang, W.; Kim, S. H.; and Lee, D. H., "Seismic Performance of Self-Sustaining Precast Wide Beam-Column Connections for Fast-Built Construction," *Computers and Concrete*, V. 33, No. 3, 2023, pp. 339-349.

14. Kim, J. H.; Lee, D. H.; Choi, S. H.; Jeong, H. S.; and Kim, K. S., "Seismic Performance of Precast Multi-Span Frame System Integrated by Unbonded Tendons," *ACI Structural Journal*, V. 119, No. 5, Sept. 2022, pp. 193-206.

15. Hwang, J. H.; Choi, S. H.; Lee, D. H.; Kim, K. S.; and Kwon, O. S., "Seismic Behavior of Post-Tensioned Precast Concrete Beam-Column Connections," *Magazine of Concrete Research*, V. 73, No. 9, 2021, pp. 433-447.

16. ACI Committee 318, "Building Code Requirements for Structural Concrete (ACI 318-19) and Commentary (ACI 318R-19) (Reapproved 2022)," American Concrete Institute, Farmington Hills, MI, 2019, 624 pp.

17. Hawkins, N. M., and Ghosh, S. K., "Shear Strength of Hollow-Core Slabs," *PCI Journal*, V. 51, No. 1, 2006, pp. 110-115.

18. Palmer, K. D., and Schultz, A. E., "Factors Affecting Web-Shear Capacity of Deep Hollow-Core Units," *PCI Journal*, V. 55, No. 2, 2010, pp. 123-146.

19. Palmer, K. D., and Schultz, A. E., "Experimental Investigation of the Web-Shear Strength of Deep Hollow-Core Units," *PCI Journal*, V. 56, No. 3, 2011, pp. 83-104.

20. El-Sayed, A. K.; Al-Negheimish, A. I.; and Alhozaimy, A. M., "Web Shear Resistance of Prestressed Precast Deep Hollow Core Slabs," *ACI Structural Journal*, V. 116, No. 1, Jan. 2019, pp. 139-150.

21. McDermott, M. R., and Dymond, B. Z., "Shear Capacity of Hollow-Core Slabs with Concrete-Filled Cores," *PCI Journal*, V. 65, No. 2, 2020, pp. 59-74.

22. Asperheim, S. A., and Dymond, B. Z., "Factors Affecting the Web-Shear Capacity of Hollow-Core Slabs with Filled Cores," *PCI Journal*, V. 66, No. 4, 2021, pp. 43-65.

23. Kim, S. Y.; Lee, D. H.; Oh, J. H.; and Han, S. J., "Effect of Cast-in-Place Concrete and Stirrups on Shear Capacity of Precast Composite Hollow-Core Slabs," *ACI Structural Journal*, V. 121, No. 6, Nov. 2024, pp. 75-90.

24. Precast/Prestressed Concrete Institute (PCI), *PCI Design Handbook*, eighth edition, Chicago, IL, 2017.

25. Corney, S. R.; Puranam, A.; Elwood, K. J.; Henry, R. S.; and Bull, D., "Seismic Performance of Precast Concrete Hollow-Core Floors: Part 1-Experimental Data," *ACI Structural Journal*, V. 118, No. 5, Sept. 2021, pp. 49-63.

26. Sarkis, A. I.; Sullivan, T. J.; Brunesi, E.; and Nascimbene, R., "Investigating the Effect of Bending on the Seismic Performance of Hollow-Core Flooring," *International Journal of Concrete Structures and Materials*, V. 17, No. 1, 2023, pp. 1-12.

27. Lee, D. H.; Yerzhanov, M.; Ju, H.; Shin, H.; and Kang, T. H.-K., "Modification of Approximate Method of ACI 318 Prestressed Concrete Shear Provision," *ACI Structural Journal*, V. 120, No. 3, May 2023, pp. 131-144.

28. Ju, H.; Yerzhanov, M.; Lee, D. H.; Shin, H.; and Kang, T. H.-K., "Modifications to ACI 318 Shear Design Method for Prestressed Concrete Members: Detailed Method," *PCI Journal*, V. 68, No. 1, 2023, pp. 60-85.

29. Kang, T. H.-K.; Lee, D. H.; Yerzhanov, M.; and Ju, H., "ACI 318 Shear Design Method for Prestressed Concrete Members - Proposed Modifications," *Concrete International*, V. 43, No. 10, Oct. 2021, pp. 42-50.

30. Bondy, K. D., and Bondy, K. B., "Shear Nonsense …," *Concrete International*, V. 38, No. 10, Oct. 2016, pp. 51-56.

31. Kim, C. G.; Park, H. G.; Hong, G. H.; Lee, H. R.; and Suh, J. I., "Shear Strength of Reinforced Concrete-Composite Beams with Prestressed Concrete and Non-Prestressed Concrete," *ACI Structural Journal*, V. 115, No. 4, July-Aug. 2017, pp. 917-930.

32. Kim, C. G.; Park, H. G.; Hong, G. H.; and Kang, S. M., "Shear Strength of Composite Beams with Dual Concrete Strengths," *ACI Structural Journal*, V. 113, No. 2, Mar.-Apr. 2016, pp. 263-274.

33. Kim, C. G.; Park, H. G.; Hong, G. H.; Kang, S. M.; and Lee, H. R., "Shear Strength of Concrete Composite Beams with Shear Reinforcements," *ACI Structural Journal*, V. 114, No. 4, July-Aug. 2017, pp. 827-837.

34. Park, M. K.; Lee, D. H.; Ju, H.; Hwang, J. H.; Choi, S. H.; and Kim, K. S., "Minimum Shear Reinforcement Ratio of Prestressed Concrete Members for Safe Design," *Structural Engineering and Mechanics*, V. 56, No. 2, 2015, pp. 317-340.

35. Lee, J. Y., and Kim, U. Y., "Effect of Longitudinal Tensile Reinforcement Ratio and Shear Span-Depth on Minimum Shear Reinforcement in Beams," *ACI Structural Journal*, V. 105, No. 2, Mar.-Apr. 2008, pp. 134-144.

36. Teoh, B. K.; Mansur, M. A.; and Wee, T. H., "Behavior of High-Strength Concrete I-Beams with Low Shear Reinforcement," *ACI Structural Journal*, V. 99, No. 3, May-June 2002, pp. 299-307.

37. Walraven, J. C., and Mercx, W. P. M., "The Bearing Capacity for Prestressed Hollow Core Slabs," *Heron*, V. 28, No. 3, 1983, pp. 1-46.

38. Pajari, M., "Resistance of Prestressed Hollow Core Slabs Against Web Shear Failure," Technical Research Centre of Finland, Espoo, Finland, 2005.

39. TNO Building and Constructions Research, TNO Report: Standard Shear Tests on Prestressed Hollow Core Slabs According to EN 1168, TNO Building and Constructions Research, Hague, the Netherlands, 2005.

40. Bertagnoli, G., and Mancini, G., "Failure Analysis of Hollow-Core Slabs Tested in Shear," *Structural Concrete*, V. 10, No. 3, 2009, pp. 139-152.

41. Prefabbricati, G., "Static Load Tests on Spiroll Hollow-Core Slabs," University of L'Aquila, L'Aquila, Italy, 2003.

42. Celal, M. S., "Shear Behaviour of Precast/Prestressed Hollow-Core Slabs," MSc dissertation, University of Manitoba, Winnipeg, MB, Canada, 2011.

43. Rahman, M. K.; Baluch, M. H.; Said, M. K.; and Shazali, M. A., "Flexural and Shear Strength of Prestressed Precast Hollow-Core Slabs," *Arabian Journal for Science and Engineering*, V. 37, No. 2, 2012, pp. 443-455.

44. Simasathien, S.; and Chao, S., "Shear Strength of Steel-Fiber-Reinforced Deep Hollow-Core Slabs," *PCI Journal*, V. 60, No. 4, 2015, pp. 85-101.

APPENDIX A - Examples: PHCS with cast-in-place concrete in negative moment region

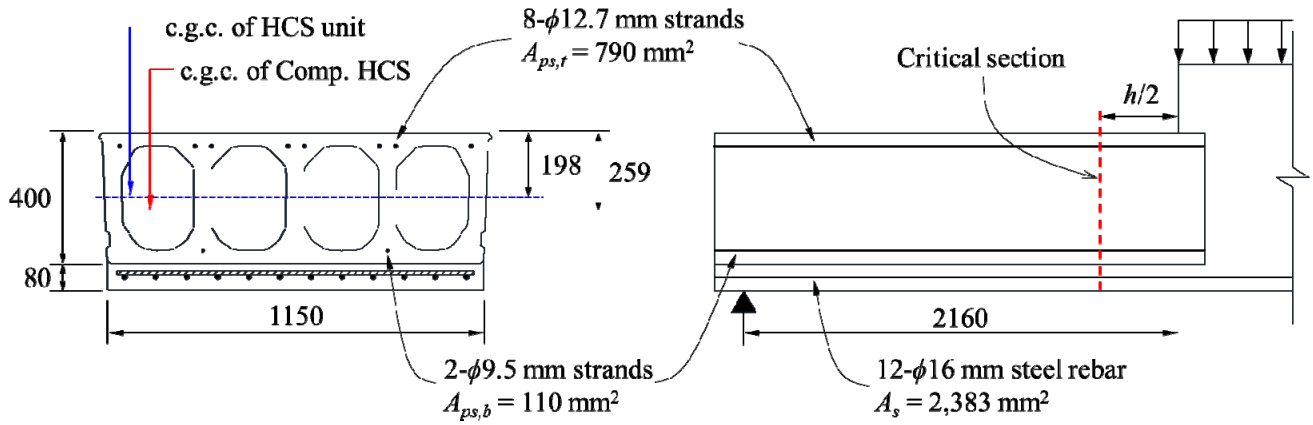

Fig. A1 Section properties and geometrical information

Prestressed hollow-core slab unit

Dimensions:
h_{HCS} = 400 mm
b_w = 276 mm
L = 5,020 mm
a = 2,160 mm
$A_{g,HCS}$ = 212,114 mm^2
$I_{g,HCS}$ = 4.408×10^9 mm^4
$y_{b,HCS}$ = 197.9 mm
$e_{p,HCS}$ = 118.8 mm

Concrete:
$f_{c,HCS}'$ = 60.5 MPa
$E_{c,HCS}$ = 33,370 MPa

Reinforcing steel:
f_{pu} = 1,860 MPa
f_{py} = 1,674 MPa
f_{se} = 0.65·f_{pu} = 1,206 MPa
f_y = 400 MPa
E_s = 200,000 MPa

Composite PHCS (transformed section using $E_{c,CIP}$ /$E_{c,HCS}$ ratio)

Dimensions:
h_{CIP} = 80 mm
$A_{g,comp}$ = 283,577 mm^2
$y_{b,comp}$ = 221.1 mm
$I_{g,comp}$ = 7.578×10^9 mm^4

Concrete:
$f_{c,CIP}'$ = 28.4 MPa
$E_{c,CIP}$ = 25,921 MPa
$E_{c,CIP}$ /$E_{c,HCS}$ = n = 0.78

Case 1: Flexure-shear strength V_{ci} of PHCS unit

At the critical section located at h/2 away from the loading point, the effective depth of prestressing steel (d_p) can be taken, as follows:

$$d_p = 360 (= 0.8h)$$

Effective prestressing force (P_e) within the transfer length (l_t) can be calculated, as follows:

$$l_t = 50 \cdot d_b = 50 \times 12.7 = 635\,\text{mm}$$

$$P_e = \frac{(h/2+80)}{l_t} f_{pe} \cdot \left(A_{ps,b} + A_{ps,t} \right) = \frac{320}{635} \times 1,206 \times (110 + 789.6) = 546.73\,\text{kN}$$

$$f_{pe,t} = \frac{P_e}{A_{g,HCS}} + \frac{P_e e_{p,HCS}}{I_{g,HCS}} y_{b,HCS} = \frac{546.73\,\text{kN}}{212{,}114\,\text{mm}^2} + \frac{546.73\,\text{kN} \times 118.8\,\text{mm}}{4.408 \times 10^9\ \text{mm}^4} 197.9\,\text{mm} = 5.50\,\text{MPa (compression)}$$

$$f_{pe,b} = \frac{P_e}{A_{g,HCS}} + \frac{P_e e_{p,HCS}}{I_{g,HCS}} y_{t,HCS} = \frac{546.73\,\text{kN}}{212{,}114\,\text{mm}^2} - \frac{546.73\,\text{kN} \times 118.8\,\text{mm}}{4.408 \times 10^9\ \text{mm}^4} (400 - 197.9\,\text{mm}) = -0.40\,\text{MPa (tension)}$$

where the seating length of PHCS is 80 mm. The shear and moment due to self-weight can be estimated, as follows:

$$DL_{HCS} = A_{g,HCS} \times 24.5\,\text{kN/m}^3 = 5.20\ \text{kN/m}$$

$$V_d = \frac{1}{2} \times (5.20\,\text{kN/m} \times 5.02\,\text{m}) - 5.20\,\text{kN/m} \times (2.16\,\text{m} - 0.24\,\text{m}) = 3.07\ \text{kN}$$

$$M_d = \frac{1}{2} \times (5.20\,\text{kN/m} \times 5.02\,\text{m}) \times (2.16\,\text{m} - 0.24\,\text{m}) - \frac{1}{2} \times 5.20\,\text{kN/m} \times (2.16\,\text{m} - 0.24\,\text{m})^2 = 15.47\ \text{kN} \cdot \text{m}$$

On this basis, the tensile stress due to self-weight (f_d) can be computed, as follows:

$$f_d = \frac{M_d}{I_{g,HCS}} y_b = \frac{15.47\,\text{kN} \cdot \text{m}}{4.408 \times 10^9\ \text{mm}^4} \times (400 - 197.9\,\text{mm}) = 0.71\,\text{MPa}$$

On this basis, cracking moment (M_{cre}) can be estimated, as follows:

$$M_{cre} = \frac{I_{g,HCS}}{(h - y_b)} \left(0.5\sqrt{f_{c,HCS}'} + f_{pe,b} - f_d \right) = \frac{4.408 \times 10^9\ \text{mm}^4}{(400 - 197.9\,\text{mm})} \times \left(0.5\sqrt{60.5} + 0.40 - 0.71 \right) = 60.6\ \text{kN} \cdot \text{m}$$

Shear and moment due to factored loads are:

$$V_i = V_u - V_d$$

$$M_{\max} = M_u - M_d$$

For calculating flexure-shear strength (V_{ci}), some iterative calculations are required, and detailed process can be found in elsewhere (Kang et al. 2021, Bondy and Bondy 2016). On this basis, $V_{ci} = V_u = 75.6\,\text{kN}$, and then the flexure-shear strength can be estimated, as follows:

$$V_{ci} = 0.05\lambda\sqrt{f_{c,HCS}'}\,b_w d_p + V_d + \frac{(V_u - V_d)M_{cre}}{(M_u - M_d)}$$

$$= 0.05\sqrt{60.5}\times 276\,\text{mm}\times 360\,\text{mm} + 3.07\,\text{kN} + \frac{(75.6\,\text{kN} - 3.07\,\text{kN})\times 60.6\,\text{kN}\cdot\text{m}}{\left[75.6\,\text{kN}\times(2.16\,\text{m} - 0.24\,\text{m}) - 15.47\,\text{kN}\cdot\text{m}\right]} = 75.6\,\text{kN}$$

where V_{ci} no need to be taken less than $0.17\lambda\sqrt{f_c'}\,b_w d_p$, and thus:

$$V_{ci} = 75.6\,\text{kN} > 131.4\,\text{kN}\left(= 0.17\sqrt{60.5}\times 276\,\text{mm}\times 360\,\text{mm}\right)$$

V_{ci} is governed by V_{min}, and thus V_{ci} can be taken as 131.4 kN.

Case 2: Flexure-shear strength V_{ci} of composite PHCS section

Effective depth (d_F) of the composite HCPS section under negative moment can be estimated, as follows:

$$d_p = \frac{\left(A_s f_y d_s + A_{ps} f_{se} d_p\right)}{\left(A_s f_y + A_{ps} f_{se}\right)} = \frac{(2{,}383.2\times 400\times 440 + 110\times 1206\times 360)}{(2{,}383.2\times 400 + 110\times 1206)} = 430.2\ \text{mm} > 384\,\text{mm}\,(0.8h)$$

Topping concrete of composite PHCS member in tension is nonprestressed, and thus $f_{pe,b}$ term can be taken as 0 MPa. Shear (V_d) and flexural moment (M_d) induced from self-weight can be estimated, as follows:

$$DL_{HCS} + DL_{CIP} = \left(A_{g,HCS} + A_{g,CIP}\right)\times 24.5\,\text{kN/m}^3 = 7.45\,\text{kN/m}$$

$$V_d = \frac{1}{2}\times(45.12\,\text{kN}) - 7.45\,\text{kN/m}\times(2.16\,\text{m} - 0.24\,\text{m}) = 8.26\ \text{kN}$$

$$M_d = \frac{1}{2}\times(45.12\,\text{kN})\times(2.16\,\text{m} - 0.24\,\text{m}) - \frac{1}{2}\times 7.45\,\text{kN/m}\times(2.16\,\text{m} - 0.24\,\text{m})^2 = 29.58\ \text{kN}\cdot\text{m}$$

As the critical section, tensile stress (f_d) induced by M_d and corresponding M_{cre} can be computed:

$$f_d = \frac{M_d}{I_{g,comp}} y_{b,comp} = \frac{29.58\,\text{kN}\cdot\text{m}}{7.578\times10^9\ \text{mm}^4}\times 221.1\,\text{mm} = 0.86\,\text{MPa}$$

$$M_{cre} = \frac{I_{g,comp}}{y_{b,comp}}\left(0.5\sqrt{f_c'} + f_{pe,b} - f_d\right) = \frac{7.578\times10^9\ \text{mm}^4}{221.1\,\text{mm}}\times\left(0.5\sqrt{28.4} + 0 - 0.86\right) = 61.69\ \text{kN}\cdot\text{m}$$

Shear and moment due to factored loads are:

$$V_i = V_u - V_d$$

$$M_{\max} = M_u - M_d$$

For calculating flexure-shear strength (V_{ci}), some iterative calculations are required, and detailed process can be found in elsewhere (Kang et al. 2021, Bondy and Bondy 2016). On this basis, $V_{ci} = V_u = 89.7\,\text{kN}$, and then the flexure-shear strength can be estimated, as follows:

$$V_{ci} = 0.05\lambda\sqrt{f_c'}\,b_w d_p + V_d + \frac{(V_u - V_d)\,M_{cre}}{(M_u - M_d)}$$

$$= 0.05\sqrt{60.5}\times 276\,\text{mm}\times 430.2\,\text{mm} + 8.26\,\text{kN} + \frac{(89.7\,\text{kN} - 8.26\,\text{kN})\times 61.69\,\text{kN}\cdot\text{m}}{\left[89.7\,\text{kN}\times(2.16\,\text{m} - 0.24\,\text{m}) - 29.58\,\text{kN}\cdot\text{m}\right]} = 89.7\,\text{kN}$$

where V_{ci} no need to be taken less than $0.17\lambda\sqrt{f_c'}\,b_w d_p$, and thus:

$$V_{ci} = 89.7\,\text{kN} > 157.0\,\text{kN}\left(= 0.17\sqrt{60.5}\times 276\,\text{mm}\times 430.2\,\text{mm}\right)$$

V_{ci} is governed by V_{min}, and thus V_{ci} can be taken as 157.0 kN.

Case 3: Web-shear strength V_{cw} of composite PHCS

Web-shear Strength (V_{cw}) takes into account the compressive stress due to prestress (f_{pc}) as a key

factor. For PHCS composite section, the centroid is inevitably changed due to CIP concrete, as presented in Fig. A1. On this basis, the f_{pc} can be estimated, as follows:

$$L_t = 50 d_{bp} = 50 \times 12.7 = 635\,\text{mm}$$

$$P_e = \frac{(h/2+80)}{L_t} f_{pe} \cdot \left(A_{ps,b} + A_{ps,t} \right) = \frac{320}{635} \times 1,206 \times (110 + 789.6) = 546.73\,\text{kN}$$

$$f_{pc,HCS} = \frac{P_e}{A_{g,HCS}} = \frac{546.73\,\text{kN}}{212,114\,\text{mm}^2} = 2.58\ \text{MPa}$$

$$f_{pc,comp} = \frac{\left(f_{pe,t} - f_{pe,b} \right)}{h_{HCS}} \left(h_{HCS} - y_{t,comp} \right) + f_{pe,b} = \frac{(5.50 + 0.40\,\text{MPa})}{400\,\text{mm}} \times (480 - 259\,\text{mm}) - 0.40\,\text{MPa} = 1.68\,\text{MPa}$$

In addition, the prestressing strand profile is straight, and thus, there is no vertical shear component of prestressing force (V_p=0). On this basis, the web-shear strength (V_{cw}) can be calculated, as follows:

$$V_{cw} = \left(0.29\lambda\sqrt{f_c'} + 0.3 f_{pc,comp} \right) b_w d_p = \left(0.29\sqrt{60.5} + 0.3 \times 1.68 \right) \times 276\,\text{mm} \times 430.2\,\text{mm} = 327.7\ \text{kN}$$

References

Kang, T. H.-K., Lee, D. H., Yerzhanov, M., and Ju, H., "ACI 318 Shear Design Method for Prestressed Concrete Members - Proposed Modifications," *Concrete International*, Vol. 43, No. 10, 2021, pp. 42-50.

Bondy, K. D., and Bondy, K. B., "Shear Nonsense …." *Concrete International*, Vol. 38, No. 10, 2016, pp. 51-56.